

# Torque reversals and wind variations of X-ray pulsar Vela X-1

Zhenxuan Liao,<sup>1,2</sup> Jiren Liu,<sup>3\*</sup> Lijun Gou<sup>2,4</sup>

<sup>1</sup>*School of Information Engineering, Sanming University, Jingdong Road 25, Sanming 365004, Fujian Province, People's Republic of China*

<sup>2</sup>*Key Laboratory for Computational Astrophysics, National Astronomical Observatory, Chinese Academy of Sciences, Datun Road 20A, Beijing 100012, People's Republic of China*

<sup>3</sup>*Beijing Planetarium, Xizhimenwai Road, Beijing 100044, China*

<sup>4</sup>*School of Astronomy and Space Science, University of Chinese Academy of Sciences, Beijing 100049, People's Republic of China*

6 October 2022

## ABSTRACT

The erratic spin history of Vela X-1 shows some continuous spin-up/spin-down trend over tens of days. We study the orbital profile and spectral property of Vela X-1 in these spin-up/spin-down intervals, using the spin history monitored by *Fermi*/GBM and light curve from *Swift*/BAT and *MAXI*/GSC. The BAT fluxes in the spin-up intervals are about 1.6 times those of the spin-down intervals for out-of-eclipse orbital phases. The spin-up intervals also show a higher column density than the spin-down intervals, indicating there are more material on the orbital scale for the spin-up intervals. It could be due to the variation of the stellar wind of the optical star (HD 77581) on tens of days. The varying wind could lead to alternating prograde/retrograde accreting flow to the neutron star, which dominates the transfer of the angular momentum to Vela X-1, but not the total observed luminosity.

**Key words:** Pulsars: individual: Vela X-1 – X-rays: binaries

## 1 INTRODUCTION

X-ray pulsars are magnetized neutron stars accreting material from their companion star and producing regular X-ray pulses due to the spin of the neutron star. Unlike radio pulsars that generally spinning down, the spin evolution of X-ray pulsars is more complicated. Many classical sources, such as Vela X-1, OAO 1657-415, GX 301-2, Cen X-3, and GX 1+4, show alternating spin-up and spin-down episodes on various timescale from days to decades, a phenomena not fully understood yet (e.g. Bildsten et al. 1997; Malacaria et al. 2020). In principle, the spin evolution of X-ray pulsars is governed by the interaction of the accreting flow with the magnetosphere and the neutron star. The complex nature of this multi-scale, multi-physics interaction hampered our understanding of the spin behavior of X-ray pulsars, especially for wind-fed systems (e.g. Martínez-Núñez et al. 2017).

In a recent study of OAO 1657-415, we found its spin frequency derivative is correlated with luminosity during spin-up periods and anti-correlated with luminosity during spin-down periods (Liao et al. 2022), similar to GX 1+4 (Chakrabarty et al. 1997). Moreover, we found that the orbital profile of OAO 1657-415 is dependent on the spin-up/spin-down state, indicating the accretion torque is related, somehow, with the property of accretion flow on the binary orbital scale. This finding motivates us to check whether the orbital behavior of other X-ray pulsars is dependent on the spin-up/spin-down state of the neutron star.

In this letter, we perform a torque-dependent study of the orbital property of Vela X-1, an archetype of wind-fed X-ray pulsar. It has a spin period of  $\sim 283$  s (McClintock et al. 1976), an orbital period of

8.9644 days (Falanga et al. 2015; Kreykenbohm et al. 2008), a tight orbital separation of  $53.4 R_{\odot}$  (van Kerkwijk et al. 1995), a low eccentricity  $e \sim 0.09$  (e.g. Boynton et al. 1986), and a moderate magnetic field around  $2.6 \times 10^{12}$  G (e.g. Kretschmar et al. 1996). Its optical companion, HD 77581, is an early-type B supergiant. Many properties of Vela X-1 system was recently reviewed by Kretschmar et al. (2021).

## 2 OBSERVATIONS

On-board *Fermi* Gamma-ray Space Telescope, Gamma-ray Burst Monitor (GBM) is an unfocused and all-sky instrument, well suitable for monitoring X-ray pulsars (Meegan et al. 2009). The GBM Accreting Pulsar Program (GAPP) monitors dozens of accreting pulsars and publishes frequency and pulsed flux histories on its webpage<sup>1</sup> (Malacaria et al. 2020). To measure the spin frequency of Vela X-1, the eclipsing time was excluded, and the non-eclipsing time within one orbital cycle was divided into 3 segments. The spin frequency is searched in each segment based on  $Y_n$  statistic, and the frequency with  $Y_n$  above a certain value is considered a significant detection (Finger et al. 2009).

The Burst Alert Telescope (BAT) onboard *Neil Gehrels Swift Observatory* is designed to provide critical GRB triggers with a large field of view. It has been continuously monitoring the X-ray sky in 15–200 keV band since 2005 (Krimm et al. 2013). The Monitor of All-sky X-ray Image (*MAXI*) is an high energy astrophysical experiment deployed on International Space Station in 2009. Its Gas Slit Camera (GSC, Mihara et al. 2011) has been continuously monitoring

\* Email: liujiren@bjp.org.cn

<sup>1</sup> <https://gamma-ray.msfc.nasa.gov/gbm/science/pulsars>

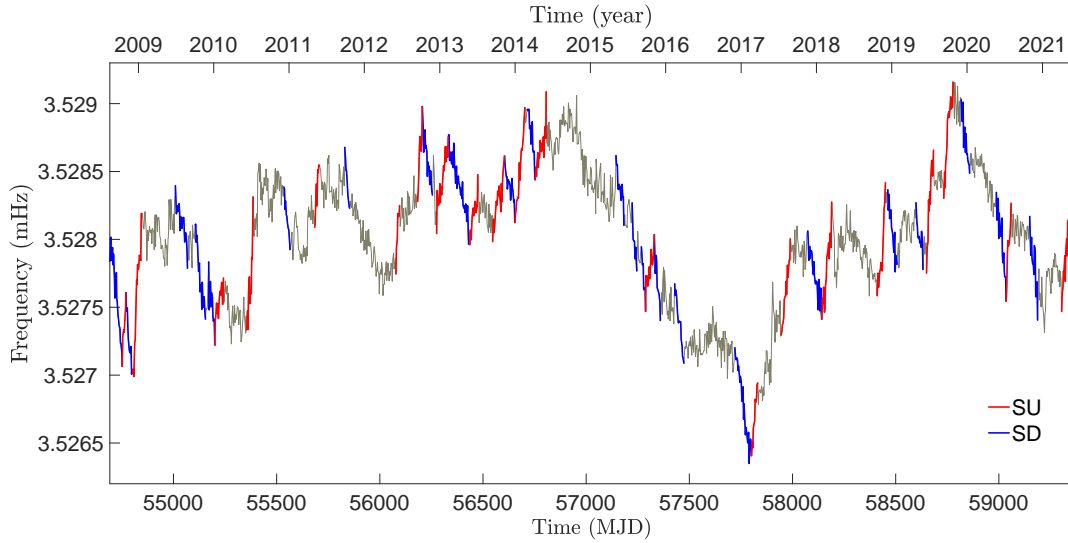


**Figure 1.** Decade-long spin frequency history of Vela X-1 monitored by *Fermi*/GBM, with the selected SU (red) and SD (blue) intervals for following analysis.

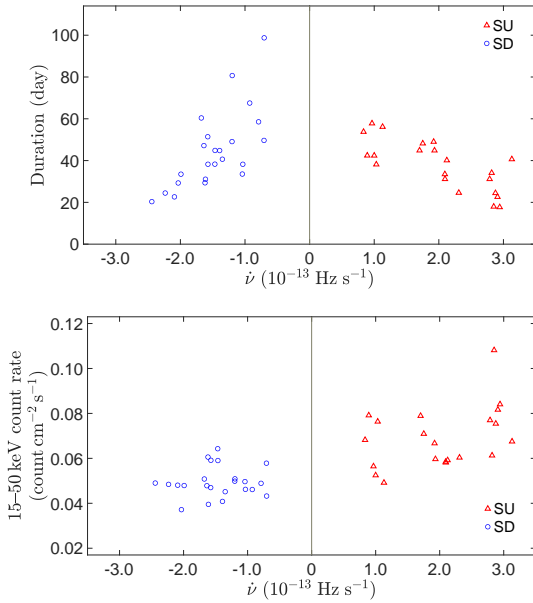


**Figure 2.** The duration (top) and BAT flux (bottom) versus the spin changing rate for SU/SD intervals.

the whole sky in 2–20 keV band. To study the long-term spin behavior of Vela X-1, we analyze the spin history of Vela X-1 monitored by GAPP, together with the corresponding light curves from *Swift*/BAT and *MAXI*/GSC.

### 3 RESULTS

The spin frequency of Vela X-1 monitored by *Fermi*/GBM, together with the pulsed flux, is presented in Figure 1. As can be seen, the spin frequency varies on the shortest timescale of measurement. The erratic spin variations of Vela X-1 had been found to be consistent with a random walk in pulse frequency (Deeter et al. 1989). On the other hand, its spin history also shows some continuous spin-up/spin-down trend over tens of days. These continuous spin-up/spin-

down periods have been pointed out by Malacaria et al. (2020) and Kretschmar et al. (2021) and been discussed roughly in a general sense. Here we perform a detailed analysis of these periods. To analyze the spin-up (SU) and spin-down (SD) episodes separately, we first select, by eye, all apparently continuous SU/SD intervals longer than 2 orbital period (17.93 days). Then we find that most of the selected intervals have a change of spin frequency  $\Delta\nu > 4.5 \times 10^{-7}$  Hz and an absolute value of Pearson coefficient larger than 0.8. So we remove a few intervals not satisfying these two conditions. The selected SU/SD intervals are marked with red/blue color in Figure 1.

We calculate an average spin frequency derivative within each interval via a linear fit. The obtained rate is plotted against the duration of each interval in the left panel of Figure 2. As can be seen, the periods of SU intervals last for 20–60 days, while those of SD intervals can last for a little longer. The spin changing rates in the SD intervals are generally larger than  $-2 \times 10^{-13}$  Hz s $^{-1}$ , while the largest spin changing rate in the SU intervals reaches  $3 \times 10^{-13}$  Hz s $^{-1}$ . The absolute value of the spin changing rate seems anti-correlated with the duration of each interval, for both SU and SD intervals (with a Pearson coefficient of -0.75 and 0.69, respectively). In the right panel of Figure 2, we plot the average *Swift*/BAT flux in 15–50 keV against the spin changing rate, for the SU and SD intervals, respectively. The average BAT flux in the SU episodes is about 0.07 count cm $^{-2}$  s $^{-1}$ , a little higher than that in the SD episodes (0.05 count cm $^{-2}$  s $^{-1}$ ). It seems the BAT fluxes and spin frequency derivatives are too scattered to show a definite correlation, and the Pearson coefficient for SU/SD intervals is 0.39 and 0.09, respectively.

#### 3.1 Orbital profile

The orbital profile of Vela X-1 had been extensively studied in the literature, and it was found to be energy-dependent: the higher the energy band, the simpler the shape (e.g. Kretschmar et al. 2021). Based on the ephemeris in Falanga et al. (2015), we calculate the orbital profile of Vela X-1 for the selected SU and SD episodes separately. The soft band (2–4 keV, 4–10 keV) and the hard band (15–50 keV) profile is extracted from *MAXI*/GSC and *Swift*/BAT, respectively. The obtained profiles are presented in Figure 3. Note

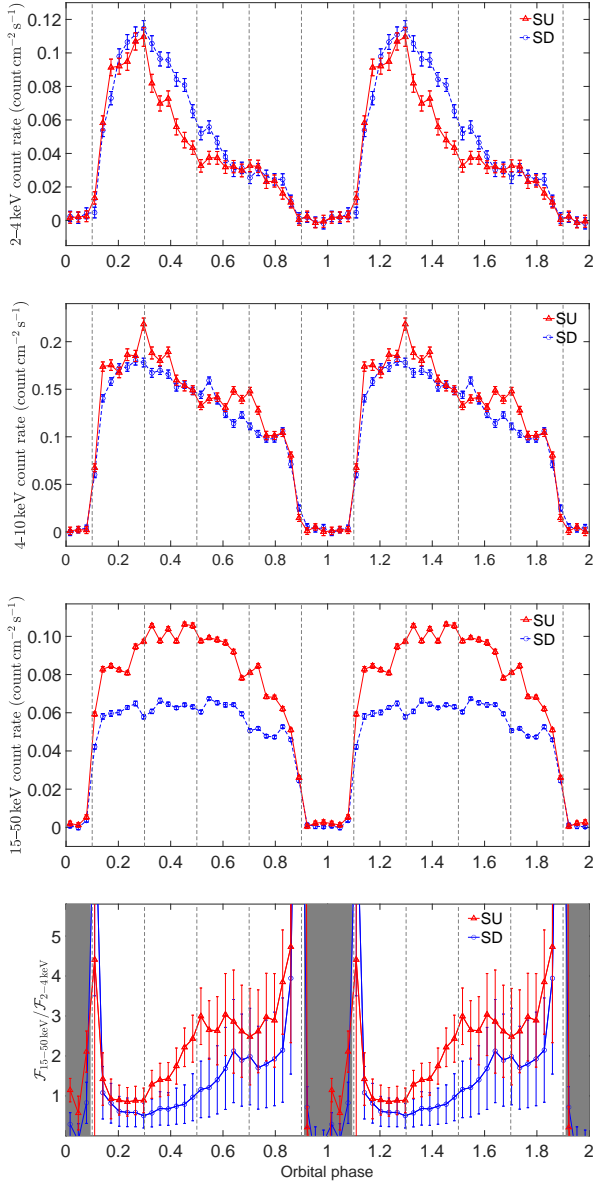


**Figure 3.** Orbital profile of Vela X-1 in soft band (2–4 keV, top; 4–10 keV, second) and hard energy band (15–50 keV, third), and the hardness ratio (bottom) for the selected SU and SD episodes. Vertical dashed lines mark the four phase bins used for spectral extraction.

that these profiles are averaged over multiple stretches of data, the individual profile of which could be quite different.

The soft band orbital profiles in 2–4 keV are peaked around phase 0.3, similar as those reported in the literature. The 2–4 keV profile of the SD intervals is a little higher (by a factor  $\sim 1.2 - 1.3$ ) than that of the SU intervals around the orbital phases of 0.2–0.6, and they look similar at other phases. The 4–10 keV profiles are also peaked around phase 0.3, but are quite similar for both the SU and SD intervals. The hard band profiles are more flat, which is also consistent with previous studies. In contrast to the soft profiles, the hard fluxes in the SD episodes are lower than those in the SU episodes, by a factor  $\sim 0.6 - 0.7$ , during the orbital phases within 0.15–0.85.

From the orbital profiles within the soft and hard bands, it can be seen that there are spectral differences between the SU and SD

episodes. The orbital hardness ratio profile between the hard and soft bands is shown in the bottom panel of Figure 3. The hardness ratio in the SU episodes is larger than that in the SD episodes for phases out of eclipse. Around the eclipse phases (shaded areas), the hardness ratio shows large fluctuation due to the very small fluxes.

### 3.2 Spectra

To further illustrate the spectral differences between different torque states, we divide the orbital phase into four bins (0.1–0.3, 0.3–0.5, 0.5–0.7, 0.7–0.9), and extract the spectrum of each phase bin from the accumulated event files provided by *MAXI*/GSC, for SU and SD intervals, respectively. The orbital-phase-resolved spectra are plotted in Figure 4. Note that these spectra are averaged over data of different periods and flux levels, and the individual spectrum could be quite different.

As can be seen, all the spectra of the SU intervals are higher than those of the SD intervals above 5 keV. While below 5 keV, the spectra of the SU intervals are apparently lower than those of the SD intervals for phases within 0.3–0.5, consistent with the results of the orbital profiles. To quantify the spectral differences, we fit a simple model of absorbed power-law (phabs  $\times$  powerlaw) to the spectra. The fitted spectra are plotted as black solid histograms in Figure 4, and the fitting parameters are listed in Table 1. For the viewing purpose, the fitted column densities and photon indexes are also plotted in Figure 5.

The obtained column densities of the SU intervals are generally higher than those of the SD intervals, which is most apparent for orbital phases between 0.3 and 0.7. This is consistent with the relatively higher hard flux and lower soft flux of the SU intervals. On the other hand, the photon indexes of the SU intervals are generally below those of the SD intervals. We note that below 3 keV, the model fluxes are lower than the observed fluxes, especially for the later orbital phases between 0.5 and 0.9. This may indicate inhomogeneous absorption and/or emergence of emission lines. The fitted column densities are a little lower than those obtained by individual spectral studies (e.g. Fig. 5 in Kretschmar et al. 2021), which may be due to the simplified modelling of the averaged spectra. Adopting a distance of 2 kpc derived from the third *Gaia* data release (Kretschmar et al. 2021), the absorption-corrected luminosity within 2–30 keV band is estimated in each orbital phase bin, and the results are listed in Table 1. The intrinsic luminosity of the SU intervals is generally higher (with a factor  $\sim 10 - 20\%$ ) than that of the SD intervals.

## 4 DISCUSSIONS AND CONCLUSIONS

Based on the long-term data monitored by *Fermi*/GBM, *Swift*/BAT and *MAXI*/GSC, we studied the orbital profile of Vela X-1, for the intervals of different torque states (SU/SD). The orbital profile of the SU intervals in 15–50 keV band is systematically higher than that of the SD intervals, while the profile of the SU intervals in 2–4 keV is lower than that of the SD intervals around phase 0.2–0.6. A detailed spectral analysis showed that the fitted column densities during the SU intervals are generally higher than those of the SD intervals, while the fitted photon indexes of the SU intervals are generally smaller than those of the SD intervals.

The torque-dependent column density came out as a surprise. The periods of selected SU/SD intervals are around 20–100 days, which are longer than the orbital period of Vela X-1 (8.9644 days). The higher column density around orbital phase 0.6–0.9 could be explained as due to a trailing stream (e.g. Doroshenko et al. 2013),

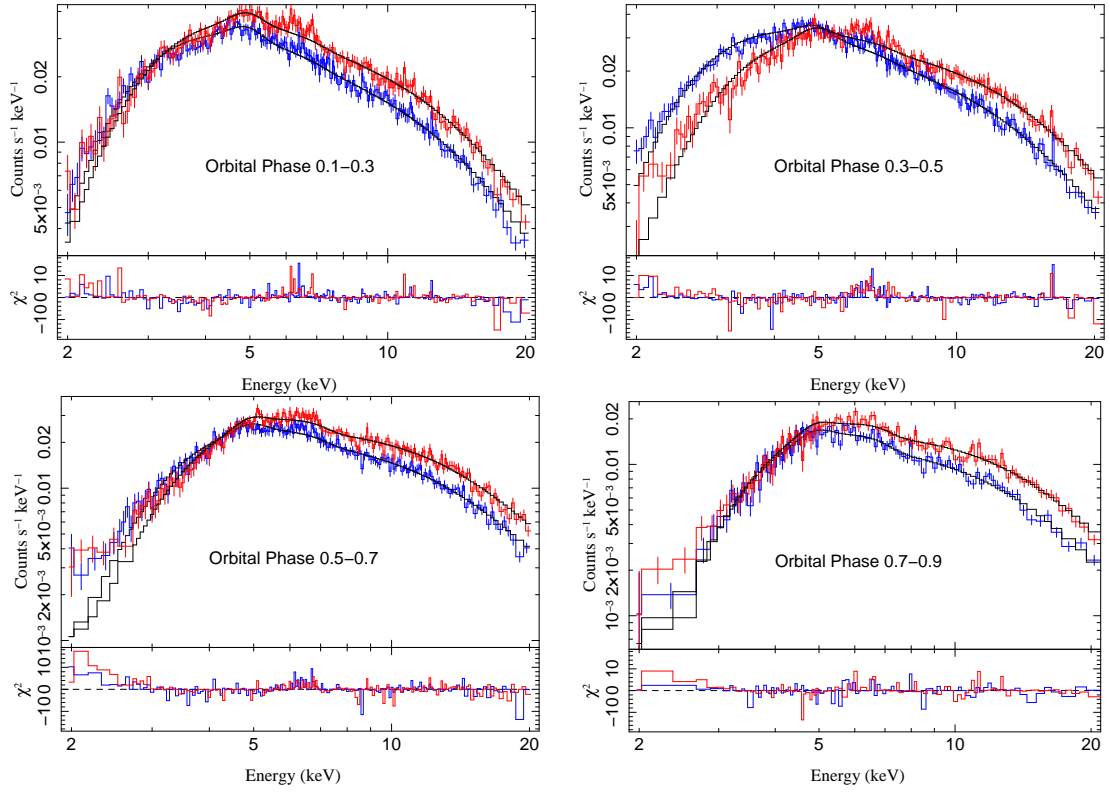


**Figure 4.** Extracted spectrum in each orbital phase bin for the SU (red) and SD (blue) episodes, together with the fitted model (black).

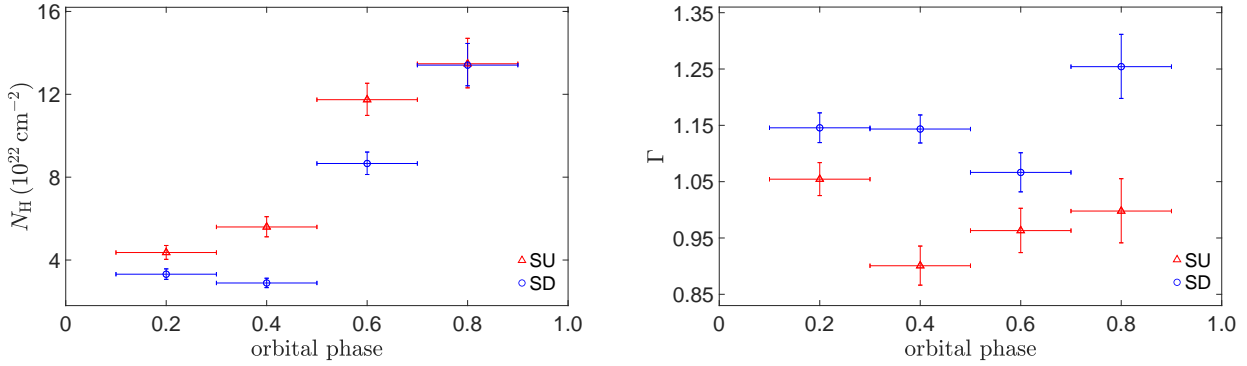


**Figure 5.** The fitted column density (left) and photon index (right) in each orbital phase bin for the SU (red) and SD (blue) episodes.

**Table 1.** Fitting results of an absorbed power-law (phabs × powerlaw). Errors are given in 90% confidence level.

$\phi_{\text{orb}}$	$N_{\text{H}} (10^{22} \text{ cm}^{-2})$	$\Gamma$	Norm <sup>1</sup>	Luminosity <sup>2</sup> ( $10^{36} \text{ erg/s}$ )	$\chi^2_{\nu}$
SD 0.1–0.3	$3.32 \pm 0.25$	$1.15 \pm 0.03$	$0.24 \pm 0.01$	$5.87 \pm 0.44$	1.32
SD 0.3–0.5	$2.89 \pm 0.23$	$1.14 \pm 0.02$	$0.23 \pm 0.01$	$5.95 \pm 0.25$	1.62
SD 0.5–0.7	$8.66 \pm 0.54$	$1.07 \pm 0.03$	$0.21 \pm 0.02$	$5.88 \pm 0.24$	1.48
SD 0.7–0.9	$13.4 \pm 1.0$	$1.25 \pm 0.06$	$0.20 \pm 0.03$	$4.25 \pm 0.19$	1.28
SU 0.1–0.3	$4.36 \pm 0.34$	$1.05 \pm 0.03$	$0.24 \pm 0.02$	$7.42 \pm 0.31$	1.53
SU 0.3–0.5	$5.60 \pm 0.49$	$0.90 \pm 0.03$	$0.17 \pm 0.02$	$7.15 \pm 0.21$	1.44
SU 0.5–0.7	$11.7 \pm 0.80$	$0.96 \pm 0.04$	$0.20 \pm 0.02$	$7.62 \pm 0.30$	1.66
SU 0.7–0.9	$13.5 \pm 1.2$	$1.00 \pm 0.06$	$0.16 \pm 0.03$	$5.17 \pm 0.27$	1.24

<sup>1</sup> Normalization of the power-law, in units of photon  $\text{keV}^{-1} \text{ cm}^{-2} \text{ s}^{-1}$  at 1 keV.

<sup>2</sup> Absorption-corrected luminosity within 2–30 keV band.



which comes into the line of sight around phase 0.5-0.6 with probable variations in individual orbit and may explain the quite different column densities found at this phase range. The fact, that the column densities of the SU intervals around both phases of 0.3 and 0.6 are higher than those of the SD intervals, indicates that there is more material between the neutron star and the earth during the SU intervals than the SD intervals, regardless of the position of the stream.

Then, the problem is on what spatial scale the enhanced/reduced material during the SU/SD intervals occurred? The involved time scale of the SU/SD intervals of 20–100 days is much longer than the dynamical time scale on the gravitational capture (Bondi) radius, also longer than the cooling time scale as involved in the quasi-spherical accretion model (Shakura et al. 2012), or the flip-flop timescale (e.g. Matsuda et al. 1987; Blondin et al. 1990). Therefore, it seems the most feasible scale of the enhanced/reduced material during the SU/SD intervals is the orbital scale. That is, the wind material itself is likely enhanced/reduced during the SU/SD intervals.

The stellar wind of massive stars is subjected to line-driven-instability (Owocki & Rybicki 1984) and is composed of small clumps (for a recent review, see Martínez-Núñez et al. 2017). Apparently, the spatial scale of the enhanced/reduced material during the SU/SD intervals is much larger than those of individual clumps. Recently, Chandra et al. (2021) reported a possible periodic variation of spin period of Vela X-1 over a time  $\sim 5.9$  years, which may be due to cyclic activity of the supergiant companion, HD 77581. The different wind material during the SU/SD intervals of Vela X-1 could also be originated from HD 77581, if its wind is varying on tens of days and part of the accreting matter has a specific angular momentum similar as that of orbital matter (Illarionov & Sunyaev 1975). The sign of the angular momentum of the accreting matter depends on whether the matter is accreted prograde or retrograde to the neutron star, which produces the observed SU/SD trend.

The recent estimations of the wind speed at the distance of Vela X-1 by Giménez-García et al. (2016) and Sander et al. (2018) were close to or even lower than the orbital velocity of Vela X-1 (see Fig. 19 in Kretschmar et al. 2021). The small wind speed will make the wind heavily affected by the orbiting neutron star and make the formation of a transient wind-fed disk possible (Karino et al. 2019; El Mellah et al. 2019; Liao et al. 2020). While the BAT flux of the SD intervals, on average, is a little lower than that of the SU intervals, the relation between BAT flux and spin frequency derivative is too scattered to show a significant correlation. This implies that the luminosity is dominated by accreted matter of negligible angular momentum, not that transferring angular momentum to the neutron star. This is a case quite different from OAO 1657-415, for which correlation/anti-correlation between the flux and spin frequency derivative is observed for SU/SD intervals. For accretion through a standard thin disk, the predicted spin-up rate of Vela X-1 is around  $8 \times 10^{-13} \text{ s}^{-2}$  for a luminosity  $\sim 6 \times 10^{36} \text{ erg s}^{-1}$  (e.g. Liao et al. 2020), about 3-5 times larger than the average value of the selected intervals. This indicates that the accretion flow of Vela X-1 should be more irregular/spherical compared with that of OAO 1657-415, as also evidenced by the more erratic spin variations of Vela X-1 than OAO 1657-415. For spin-up/spin-down rates of other accretion scenarios (such as quasi-spherical model), we refer to Kretschmar et al. (2021) for a detailed discussion.

The fitted photon indexes of the SU intervals are systematically lower than those of the SD intervals. This might be related with the interaction between the prograde/retrograde flow with the magnetic field of the neutron star, and further investigation of their connection is needed to test it.

In summary, the SU intervals of Vela X-1 show a larger luminosity/accretion rate and higher column density than the SD intervals. It could be caused by the variations of the stellar wind of HD 77581 on tens of days, which lead to alternating prograde/retrograde accreting flow to the neutron star. The prograde/retrograde flow dominates the transfer of the angular momentum to Vela X-1, but not the total observed luminosity. If this scenario is true, one may expect other observable signature of the varying stellar wind, such as the varying P-Cygni profile of UV resonance lines, in different torque states. The result indicates that the stellar wind of massive stars, besides a clumpy structure, could be variable on tens of days.

## ACKNOWLEDGEMENTS

We thank our referee for comments improving much of the manuscript. JL acknowledges the support by National Science Foundation of China (NSFC U1938113) and by the Scholar Program of Beijing Academy of Science and Technology (DZ BS202002).

## DATA AVAILABILITY

The data utilized in this article are observed by *Fermi*/GBM, *Swift*/BAT and *MAXI*/GSC and are publicly available.

## REFERENCES

- Bildsten L., et al., 1997, *ApJS*, **113**, 367
- Blondin J. M., Kallman T. R., Fryxell B. A., Taam R. E., 1990, *ApJ*, **356**, 591
- Boynton P. E., Deeter J. E., Lamb F. K., Zylstra G., 1986, *ApJ*, **307**, 545
- Chakrabarty D., et al., 1997, *ApJ*, **481**, L101
- Chandra A. D., Roy J., Agrawal P. C., Choudhury M., 2021, *MNRAS*, **508**, 4429
- Deeter J. E., Boynton P. E., Lamb F. K., Zylstra G., 1989, *ApJ*, **336**, 376
- Doroshenko V., Santangelo A., Nakahira S., Mihara T., Sugizaki M., Mat-suoka M., Nakajima M., Makishima K., 2013, *A&A*, **554**, A37
- El Mellah I., Sander A. A. C., Sundqvist J. O., Keppens R., 2019, *A&A*, **622**, A189
- Falanga M., Bozzo E., Lutovinov A., Bonnet-Bidaud J. M., Fetisova Y., Puls J., 2015, *A&A*, **577**, A130
- Finger M. H., et al., 2009, arXiv e-prints, p. arXiv:0912.3847
- Giménez-García A., et al., 2016, *A&A*, **591**, A26
- Illarionov A. F., Sunyaev R. A., 1975, *A&A*, **39**, 185
- Karino S., Nakamura K., Taani A., 2019, *PASJ*, **71**, 58
- Kretschmar P., et al., 1996, *A&AS*, **120**, 175
- Kretschmar P., et al., 2021, *A&A*, **652**, A95
- Kreykenbohm I., et al., 2008, *A&A*, **492**, 511
- Krimm H. A., et al., 2013, *ApJS*, **209**, 14
- Liao Z., Liu J., Zheng X., Gou L., 2020, *MNRAS*, **492**, 5922
- Liao Z., Liu J., Jenke P. A., Gou L., 2022, *MNRAS*, **510**, 1765
- Malacaria C., Jenke P., Roberts O. J., Wilson-Hodge C. A., Cleveland W. H., Mailyan B., GBM Accreting Pulsars Program Team 2020, *ApJ*, **896**, 90
- Martínez-Núñez S., et al., 2017, *Space Sci. Rev.*, **212**, 59
- Matsuda T., Inoue M., Sawada K., 1987, *MNRAS*, **226**, 785
- McClintock J. E., et al., 1976, *ApJ*, **206**, L99
- Meegan C., et al., 2009, *ApJ*, **702**, 791
- Mihara T., et al., 2011, *PASJ*, **63**, S623
- Owocki S. P., Rybicki G. B., 1984, *ApJ*, **284**, 337
- Sander A. A. C., Fürst F., Kretschmar P., Oskina L. M., Todt H., Hainich R., Shenar T., Hamann W. R., 2018, *A&A*, **610**, A60
- Shakura N., Postnov K., Kochetkova A., Hjalmarsdotter L., 2012, *MNRAS*, **420**, 216
- van Kerkwijk M. H., van Paradijs J., Zuiderwijk E. J., Hammerschlag-Hensberge G., Kaper L., Sterken C., 1995, *A&A*, **303**, 483